

BCSJ Award Article

Structure of Highly Concentrated Aqueous Lithium Alaninate Solutions Studied by Neutron Diffraction with $^{14}N/^{15}N$, $^{6}Li/^{7}Li$, and H/D Isotopic Substitution Methods

Yasuo Kameda,* Motoya Sasaki, Yuko Amo, and Takeshi Usuki

Department of Material and Biological Chemistry, Faculty of Science, Yamagata University, 1-4-12 Kojirakawa, Yamagata 990-8560

Received June 8, 2005; E-mail: kameda@sci.kj.yamagata-u.ac.jp

Neutron diffraction measurements have been carried out at 25 °C for aqueous 18 mol % lithium alaninate heavy water solutions, $[C^*H_3C^*H(^*ND_2)COO^*Li]_{0.18}(D_2O)_{0.82}$, in which the isotopic compositions $^{14}N/^{15}N$, H_M/D_M (H_M: methyl-hydrogen atom), and $H_{M'}/D_{M'}$ ($H_{M'}$: methine-hydrogen atom) within the alaninate ion, and $^{6}Li/^{7}Li$ for the lithium ion were changed. The hydration structures of both alaninate and lithium ions were derived from the least squares fitting analysis of observed first-order difference functions, $\Delta_N(Q)$, $\Delta_{H_M}(Q)$, $\Delta_{H_{M'}}(Q)$, and $\Delta_{Li}(Q)$. It was revealed that the amino group of the alaninate ion forms a hydrogen bond of the N···D_{w1}–O_wD_{w2} type (O_w and D_w denote water–oxygen and water–deuterium atoms, respectively) with ca. one D_2O molecule ($r_{ND_{w1}} = 2.00(1)$ Å, ∠N···D_{w1}–$O_w = 165(10)°$), and simultaneously forms hydrogen bonds of the N···OD_2 type with 1.4(1) D_2O molecules ($r_{NO} = 2.95(5)$ Å, $r_{ND} = 3.35(5)$ Å). The numbers of water molecules neighboring hydrogen atoms within the methyl- and methine-group of the alaninate ion were determined to be 0.62(1) and 0.86(9), respectively. The first coordination shell of Li^+ was found to consist of 2.42(5) D_2O molecules and 2.3(2) alaninate ions. The bond angle ∠Li^+···O_c–C (O_c: carboxyl-oxygen atom) and the dihedral angle between the plane involving atoms Li^+···O_c–C and the plane of the carboxyl group of the alaninate ion were determined to be 101(1) and 74(1)°, respectively.

The structural properties of interactions between amino acid molecules and metal ions have received a lot of attention because of their importance in extensive fields of chemical and biological sciences. A large number of crystallographic data have been accumulated for various chelate complexes of amino acids with transition-metal ions, in which the amino acid molecule coordinates as a bidentate ligand binding through both amino-nitrogen and carboxyl-oxygen atoms.[1] The complex formation of the glycinate ion with Ni^{2+}, Cu^{2+}, and Zn^{2+} in aqueous solution has been investigated by X-ray diffraction[2–4] and EXAFS[5] methods. It has been reported that the coordination of these metal complexes is also accomplished as a bidentate chelate through the N and O atoms of the glycinate ion. An X-ray diffraction study on Zn(II) complexes with the α-alaninate ion in aqueous solution has revealed that the alaninate ion exhibits bidentate coordination.[6] A relatively small number of structural investigations have reported on the interaction between alkali metal ions and amino acid molecules. According to a theoretical study on the gas-phase complexes of the glycine molecule with Li^+ and Na^+, the lowest energy species corresponds to a five-membered ring in which Li^+ and Na^+ are coordinated to both N and O atoms of the glycine molecule.[7] On the other hand, recent single crystal X-ray diffraction results of sodium nitrate–glycine (1/1) have shown that the zwitterionic glycine molecule coordinates as a monodentate ligand to the sodium ion through a carboxyl-oxygen atom of the glycine molecule.[8] The coordination structure of amino acid with the alkali metal ion in aqueous solution has not yet been reported.

In the present paper, we describe the results of TOF neutron diffraction measurements on aqueous 18 mol % lithium alaninate heavy water solutions. $^{14}N/^{15}N$, $^{6}Li/^{7}Li$, H_M/D_M, and $H_{M'}/D_{M'}$ isotopically substituted samples were employed in order to obtain information on the environmental structure around the substituted atom. Structural parameters concerning the first hydration shell of Li^+ and those of the amino-nitrogen, the methyl-hydrogen, and the methine-hydrogen atoms of the alaninate ion were determined from the least squares fitting analyses of observed first-order difference functions, $\Delta_N(Q)$, $\Delta_{Li}(Q)$, $\Delta_{H_M}(Q)$, and $\Delta_{H_{M'}}(Q)$.

Experimental

Materials. Isotopically enriched DL-$CH_3CH(^{15}NH_2)COOH$ (98.0% ^{15}N, CIL Inc.), DL-$CD_3CH(NH_2)COOH$ (98.0% methyl-D, CIL Inc.), DL-$CH_3CD(NH_2)COOH$ (98.0% methine-D, Aldrich Chemical Co.), and DL-$CH_3CH(NH_2)COOH$ (natural abundance, Nacalai Tesque, guaranteed grade), were reacted with $^{6}LiOH\cdot H_2O$ (95.0% ^{6}Li, Aldrich Chemical Co.) and $^{7}LiOH\cdot H_2O$ (99.9%

Published on the web February 10, 2006; DOI 10.1246/bcsj.79.228

Table 1. Isotopic Composition of Sample Solutions Used in This Study

	Sample	$^{14}N/\%$	$^{15}N/\%$	$^{6}Li/\%$	$^{7}Li/\%$	$H_M/\%$[a]	$D_M/\%$[a]	$H_{M'}/\%$[b]	$D_{M'}/\%$[b]
I	$[CH_3CH(^{14}ND_2)COO^7Li]_{0.18}(D_2O)_{0.82}$	99.6	0.4	0.1	99.9	100	0	100	0
II	$[CH_3CH(^{15}ND_2)COO^7Li]_{0.18}(D_2O)_{0.82}$	2.0	98.0	0.1	99.9	100	0	100	0
III	$[CH_3CH(^{14}ND_2)COO^6Li]_{0.18}(D_2O)_{0.82}$	99.6	0.4	95.0	5.0	100	0	100	0
IV	$[CD_3CH(^{14}ND_2)COO^7Li]_{0.18}(D_2O)_{0.82}$	99.6	0.4	0.1	99.9	2.0	98.0	100	0
V	$[CH_3CD(^{14}ND_2)COO^7Li]_{0.18}(D_2O)_{0.82}$	99.6	0.4	0.1	99.9	100	0	2.0	98.0

a) For methyl-hydrogen atoms of alaninate ion. b) For methine-hydrogen atom of alaninate ion.

Table 2. Mean Scattering Lengths, b_N, b_{Li}, b_{H_M}, and $b_{H_{M'}}$, of Nitrogen, Lithium, Methyl-Hydrogen, and Methine-Hydrogen Atoms, Total Cross Sections, and Number Density of Sample Solutions Scaled in the Stoichiometric Unit, $[C^*H_3C^*H(^*ND_2)COO^*Li]_{0.18}(D_2O)_{0.82}$, σ_t and ρ, Respectively

	Sample	b_N $/10^{-12}$ cm	b_{Li} $/10^{-12}$ cm	b_{H_M} $/10^{-12}$ cm[a]	$b_{H_{M'}}$ $/10^{-12}$ cm[b]	σ_t /barns[c]	ρ /Å^{-3}
I	$[CH_3CH(^{14}ND_2)COO^7Li]_{0.18}(D_2O)_{0.82}$	0.936	−0.222	−0.374	−0.374	43.160	
II	$[CH_3CH(^{15}ND_2)COO^7Li]_{0.18}(D_2O)_{0.82}$	0.650	−0.222	−0.374	−0.374	41.863	
III	$[CH_3CH(^{14}ND_2)COO^6Li]_{0.18}(D_2O)_{0.82}$	0.936	0.179	−0.374	−0.374	132.387	0.02133
IV	$[CD_3CH(^{14}ND_2)COO^7Li]_{0.18}(D_2O)_{0.82}$	0.936	−0.222	0.646	−0.374	27.432	
V	$[CH_3CD(^{14}ND_2)COO^7Li]_{0.18}(D_2O)_{0.82}$	0.936	−0.222	−0.374	0.646	37.917	

a) For methyl-hydrogen atoms of alaninate ion. b) For methine-hydrogen atom of alaninate ion. c) For incident neutron wavelength of 1.0 Å.

^{7}Li, Tomiyama Chemical Co.) in aqueous solutions. The product solutions were carefully dehydrated at 80 °C under vacuum to obtain five anhydrous lithium alaninate samples with different isotopic compositions, DL-$CH_3CH(^{14}NH_2)COO^7Li$, DL-$CH_3CH(^{15}NH_2)COO^7Li$, DL-$CH_3CH(^{14}NH_2)COO^6Li$, DL-$CD_3CH(^{14}NH_2)COO^7Li$, and DL-$CH_3CD(^{14}NH_2)COO^7Li$. Deuteration of the amino-hydrogen atoms within the alaninate ion was achieved by dissolving the anhydrous lithium alaninate into 10 times the molar quantity of D_2O (99.9% D, Aldrich Chemical Co.), followed by dehydration at 80 °C under vacuum. This procedure was repeated 4 times. The H/D isotopic compositions of the methyl- and the methine-hydrogen atoms were checked by the FT-IR method as described previously,[9] and the consistent values were confirmed with the manufacturer's specification.

The required amounts of enriched compounds, DL-$CH_3CH(^{14}ND_2)COO^7Li$, DL-$CH_3CH(^{15}ND_2)COO^7Li$, DL-$CH_3CH(^{14}ND_2)COO^6Li$, DL-$CD_3CH(^{14}ND_2)COO^7Li$, and DL-$CH_3CD(^{14}ND_2)COO^7Li$, were respectively dissolved into D_2O (99.9% D, Aldrich Chemical Co.) to prepare five kinds of aqueous 18 mol % lithium alaninate solutions with different isotopic compositions of amino-nitrogen, methyl-hydrogen, and methine-hydrogen atoms within the alaninate ion, and also the lithium ion, i.e., I: $[CH_3CH(^{14}ND_2)COO^7Li]_{0.18}(D_2O)_{0.82}$, II: $[CH_3CH(^{15}ND_2)COO^7Li]_{0.18}(D_2O)_{0.82}$, III: $[CH_3CH(^{14}ND_2)COO^6Li]_{0.18}(D_2O)_{0.82}$, IV: $[CD_3CH(^{14}ND_2)COO^7Li]_{0.18}(D_2O)_{0.82}$, and V: $[CH_3CD(^{14}ND_2)COO^7Li]_{0.18}(D_2O)_{0.82}$, respectively. The H/D ratio of the exchangeable hydrogen atoms within the sample solution, was checked by the ATR-IR method, which has been described elsewhere.[9] The ^{13}C NMR measurements were carried out on sample solutions using a JEOL α-400 spectrometer. The results did not show any indication of the polymeric species in the present sample solutions. The sample parameters used in this study are listed in Tables 1 and 2.

Neutron Diffraction Measurements. The sample solution was sealed into a cylindrical quartz cell (7.3 mm in inner diameter and 0.5 mm in thickness). TOF neutron diffraction measurements were carried out at 25 °C using a HIT-II spectrometer[10] installed at the High Energy Accelerator Research Organization (KEK), Tsukuba, Japan. Scattered neutrons (neutron waveband of $0.1 \leq \lambda \leq 5.5$ Å) were detected by 104 ^{3}He counters covering the scattering angle range of $10 \leq 2\theta \leq 157°$. The data accumulation time was ca. 11 h for each sample. Measurements were made in advance for an empty cell, background, and a vanadium rod of 8 mm in diameter.

Data Reduction. Observed scattering intensities for the sample were corrected for instrumental background, absorption of sample and cell,[11] multiple,[12] and incoherent scatterings. The coherent scattering lengths as well as the scattering and absorption cross sections for the constituent nuclei were referred to those tabulated by Sears.[13] The wavelength dependence of the total cross sections for H and D nuclei was estimated from the observed total cross sections for H_2O and D_2O, respectively.[14] The corrected intensities were converted to an absolute scale using the corrected scattering intensities from the vanadium rod. The inelasticity correction was applied by the use of the observed self-scattering intensities from the liquid null-H_2O.[15]

The first-order difference function, $\Delta_X(Q)$,[16,17] is derived from the numerical difference between scattering cross sections observed for two solutions that are identical except for the scattering length of the nucleus X. The $\Delta_X(Q)$ can be written as a linear combination of partial structure factors, $a_{Xj}(Q)$, involving contributions from the X–j pair:

$$\Delta_X(Q) = A[a_{XO}(Q) - 1] + B[a_{XD}(Q) - 1] + C[a_{XC}(Q) - 1] + D[a_{XN}(Q) - 1] + E[a_{XH_M}(Q) - 1] + F[a_{XH_{M'}}(Q) - 1] + G[a_{XLi}(Q) - 1], \quad (1)$$

where X = N, Li, H_M, and $H_{M'}$. Since the observed $\Delta_X(Q)$ from 64 sets of forward angle detectors at $10 \leq 2\theta \leq 51°$ agree well within the statistical uncertainties, they were combined at the Q-interval of 0.1 Å^{-1} and used for subsequent analyses. Coefficients A–G in Eq. 1 are evaluated respectively for $\Delta_N(Q)$ (sample I–sample II), $\Delta_{Li}(Q)$ (sample III–sample I), $\Delta_{H_M}(Q)$ (sample IV–sample I), and $\Delta_{H_{M'}}(Q)$ (sample V–sample I), which are scaled at the stoichiometric unit, $[C^*H_3C^*H(^*ND_2)COO^*Li]_x(D_2O)_{1-x}$, as follows:

Table 3. Values of the Coefficients of $a_{ij}(Q)$ in Eq. 1

Difference function	A/barns	B/barns	C/barns	D/barns	E/barns	F/barns	G/barns
$\Delta_N(Q)$	0.0705	0.1371	0.0369	0.0147	−0.0208	−0.0069	−0.0041
$\Delta_{Li}(Q)$	0.0987	0.1921	0.0517	0.0243	−0.0291	−0.0097	−0.0006
$\Delta_{H_M}(Q)$	0.7545	1.4678	0.3954	0.1856	0.0810	−0.0742	−0.0440
$\Delta_{H_{M'}}(Q)$	0.2515	0.4893	0.1318	0.0619	−0.0742	0.0090	−0.0147

$$A = 2x(1+x)(b_{^{14}N} - b_{^{15}N})b_O,\ B = 4x(b_{^{14}N} - b_{^{15}N})b_D,$$
$$C = 6x^2(b_{^{14}N} - b_{^{15}N})b_C,\ D = x^2(b_{^{14}N}{}^2 - b_{^{15}N}{}^2),$$
$$E = 6x^2(b_{^{14}N} - b_{^{15}N})b_{H_M},\ F = 2x^2(b_{^{14}N} - b_{^{15}N})b_{H_{M'}},\ \text{and}$$
$$G = 2x^2(b_{^{14}N} - b_{^{15}N})b_{Li},\ \text{for}\ \Delta_N(Q),$$

$$A = 2x(1+x)(b_{^6Li} - b_{^7Li})b_O,\ B = 4x(b_{^6Li} - b_{^7Li})b_D,$$
$$C = 6x^2(b_{^6Li} - b_{^7Li})b_C,\ D = 2x^2(b_{^6Li} - b_{^7Li})b_N,$$
$$E = 6x^2(b_{^6Li} - b_{^7Li})b_{H_M},\ F = 2x^2(b_{^6Li} - b_{^7Li})b_{H_{M'}},\ \text{and}$$
$$G = x^2(b_{^6Li}{}^2 - b_{^7Li}{}^2),\ \text{for}\ \Delta_{Li}(Q),$$

$$A = 6x(1+x)(b_{D_M} - b_{H_M})b_O,\ B = 12x(b_{D_M} - b_{H_M})b_D,$$
$$C = 18x^2(b_{D_M} - b_{H_M})b_C,\ D = 6x^2(b_{D_M} - b_{H_M})b_N,$$
$$E = 9x^2(b_{D_M}{}^2 - b_{H_M}{}^2),\ F = 6x^2(b_{D_M} - b_{H_M})b_{H_{M'}},\ \text{and}$$
$$G = 6x^2(b_{D_M} - b_{H_M})b_{Li},\ \text{for}\ \Delta_{H_M}(Q),$$

and

$$A = 2x(1+x)(b_{D_{M'}} - b_{H_{M'}})b_O,\ B = 4x(b_{D_{M'}} - b_{H_{M'}})b_D,$$
$$C = 6x^2(b_{D_{M'}} - b_{H_{M'}})b_C,\ D = 2x^2(b_{D_{M'}} - b_{H_{M'}})b_N,$$
$$E = 6x^2(b_{D_{M'}} - b_{H_{M'}}),\ F = x^2(b_{D_{M'}}{}^2 - b_{H_{M'}}{}^2),\ \text{and}$$
$$G = 2x^2(b_{D_{M'}} - b_{H_{M'}})b_{Li},\ \text{for}\ \Delta_{H_{M'}}(Q).$$

Numerical values A–G for the respective difference functions are listed in Table 3. The distribution function, $G_X(r)$, is deduced from the Fourier transform of $\Delta_X(Q)$:

$$\begin{aligned} G_X(r) &= 1 + (A+B+C+D+E+F+G)^{-1}(2\pi^2\rho r)^{-1} \\ &\quad \times \int_{Q_{min}}^{Q_{max}} Q\Delta_X(Q)\sin(Qr)\mathrm{d}Q \\ &= [Ag_{XO}(r) + Bg_{XD}(r) + Cg_{XC}(r) + Dg_{XN}(r) \\ &\quad + Eg_{XH_M}(r) + Fg_{XH_{M'}}(r) + Gg_{XLi}(r)] \\ &\quad \times (A+B+C+D+E+F+G)^{-1}. \end{aligned} \tag{2}$$

The upper limit of the integral, Q_{max}, was set to be 20 Å^{-1} in the present study.

Structural parameters concerning the coordination shell of the X atom were obtained through the least squares fitting procedure applying the following model function:[18–20]

$$\begin{aligned} \Delta_{X^{model}}(Q) &= \sum 2c_X n_{X\alpha} b_\alpha (b_X - b_{X'}) \exp(-l_{X\alpha}{}^2 Q^2/2) \\ &\quad \times \sin(Qr_{X\alpha})/(Qr_{X\alpha}) + 4\pi\rho(A+B+C \\ &\quad + D+E+F+G)\exp(-l_{0X}{}^2 Q^2/2) \\ &\quad \times [Qr_{0X}\cos(Qr_{0X}) - \sin(Qr_{0X})]Q^{-3}, \end{aligned} \tag{3}$$

where c_X and $n_{X\alpha}$ are the number of X atoms in the stoichiometric unit and the coordination number of α atoms around the X atom, respectively. Parameters $l_{X\alpha}$ and $r_{X\alpha}$ denote the root-mean-square amplitude and internuclear distance of the X–α pair, respectively. The long-range parameter, r_{0X}, means the distance beyond which the continuous distribution of atoms around the X atom can be assumed. The parameter, l_{0X}, describes the sharpness of the boundary at r_{0X}. Structural parameters $n_{X\alpha}$, $l_{X\alpha}$, $r_{X\alpha}$, l_{0X}, and r_{0X}, are determined from the least squares fit to the observed $\Delta_X(Q)$. The fitting procedure was performed in the range of $0.6 \le Q \le 20$ Å^{-1} ($0.3 \le Q \le 12$ Å^{-1} in the case of $\Delta_N(Q)$) with the SALS program,[21] assuming that the statistical uncertainties distribute uniformly. Prior to the fitting analysis, correction for the low-frequency systematic error involved in the observed $\Delta_X(Q)$ was adopted.[22]

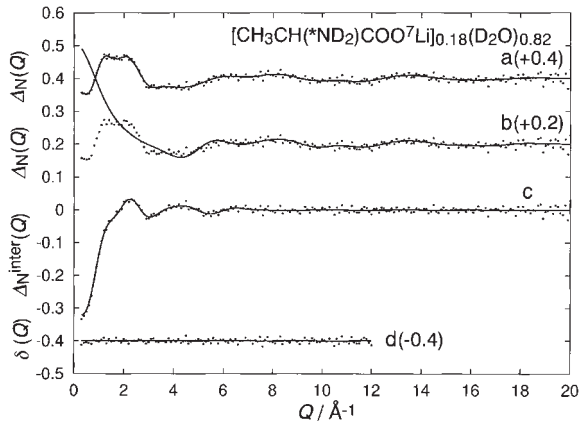

Fig. 1. a) Observed difference function, $\Delta_N(Q)$, for aqueous 18 mol % lithium alaninate heavy water solutions (dots). Smoothed $\Delta_N(Q)$, which is used for the Fourier transform (solid line). b) Observed $\Delta_N(Q)$ (dots), and the intramolecular interference term within the alaninate ion, $I_N{}^{intra}(Q)$ (solid line). c) Intermolecular difference function, $\Delta_N{}^{inter}(Q)$ (dots). The best-fit of the calculated $\Delta_N{}^{model}(Q)$ is shown by the solid line. d) The residual function, $\delta(Q)$ (dots).

In the present analysis for $\Delta_N(Q)$, $\Delta_{H_M}(Q)$, and $\Delta_{H_{M'}}(Q)$, intramolecular contribution within the alaninate ion was subtracted from the observed difference functions. The intramolecular interference term, $I_X{}^{intra}(Q)$, was estimated by the following equation:

$$\begin{aligned} I_X{}^{intra}(Q) &= \gamma \times \sum 2c_X b_\alpha (b_X - b_{X'}) \\ &\quad \times \exp(-l_{X\alpha}{}^2 Q^2/2)\sin(Qr_{X\alpha})/(Qr_{X\alpha}), \end{aligned} \tag{4}$$

where γ is the normalization factor. Values $l_{X\alpha}$ and $r_{X\alpha}$ were referred to those reported in the literature.[23,24] The calculated $I_X{}^{intra}(Q)$ was then subtracted from the corrected $\Delta_X(Q)$ to deduce the intermolecular difference function, $\Delta_X{}^{inter}(Q)$:

$$\Delta_X{}^{inter}(Q) = \Delta_X(Q) - I_X{}^{intra}(Q). \tag{5}$$

The intermolecular distribution function, $G_X{}^{inter}(r)$, was obtained by a Fourier transform of the $\Delta_X{}^{inter}(Q)$ using Eq. 2 with the upper limit of the integral, $Q_{max} = 20$ Å^{-1}.

Results and Discussion

Hydration Structure around the Amino-Nitrogen Atom. The observed difference function, $\Delta_N(Q)$, is shown in Fig. 1a.

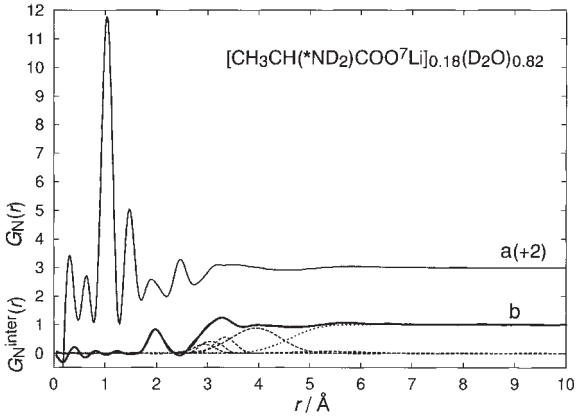

Fig. 2. a) Total distribution function around the amino-nitrogen atom, $G_N(r)$, observed for aqueous 18 mol % lithium alaninate solutions. b) Observed intermolecular distribution function, $G_N^{inter}(r)$ (thick solid line), and the Fourier transform of the calculated $\Delta_N^{model}(Q)$ (Fig. 1c) is shown by thin solid line. Short- and long-range contributions are denoted by broken and dotted lines, respectively.

The partially resolved first diffraction peak at $Q \approx 2\,\text{Å}^{-1}$ and the oscillational feature of the $\Delta_N(Q)$ extending to the higher-Q region are clearly observed. The calculated intramolecular interference term, $I_N^{intra}(Q)$ (Fig. 1b), was subtracted from the observed $\Delta_N(Q)$. The normalization factor, γ, determined by $I_N^{intra}(Q) = \gamma \times \Delta_N(Q)$ (in the sufficiently high-Q region) was obtained to be $\gamma = 0.99 \pm 0.01$ from the least squares fit in the range of $6 \leq Q \leq 20\,\text{Å}^{-1}$. The result implies that the present data correction and normalization procedures have been adequately carried out; the overall normalization error in the present $\Delta_N(Q)$ is roughly estimated to be ca. 1%. The intermolecular difference function, $\Delta_N^{inter}(Q)$ (Fig. 1c), is characterized by the first peak at $Q \approx 2\,\text{Å}^{-1}$ with a shoulder in the lower-Q side.

The total and intermolecular distribution functions, $G_N(r)$ and $G_N^{inter}(r)$, are represented in Figs. 2a and 2b, respectively. A dominant first peak at $r \approx 1.0$ Å in the total $G_N(r)$ is assigned to the intramolecular N–D interaction within the alaninate ion. The second peak at $r \approx 1.5$ Å is attributable to the intramolecular N–C_α (C_α: α-carbon atom) interaction. The sum of interactions from intramolecular N···C_M and N···C_O (C_M: methyl-carbon, C_O: carboxyl-carbon atoms, respectively) pairs can be seen as the third peak at $r \approx 2.4$ Å. The Fourier transform of the $\Delta_N^{inter}(Q)$, $G_N^{inter}(r)$, is represented in Fig. 2b. The $G_N^{inter}(r)$ is characterized by a well-resolved first peak at $r \approx 2.0$ Å and partially resolved peak at $r \approx 3.3$ Å. In the preliminary analysis, the area of the first peak was found to correspond to ca. one deuterium atom. Assuming that the nitrogen atom of the alaninate ion forms a hydrogen bond of the N···D_{W1}–$O_W D_{W2}$ type, which has been observed in the aqueous 2 mol % glycine solutions in alkaline condition,[25] the oxygen atom of the nearest neighbor D_2O molecule is expected to be located at $r \approx 3$ Å. In fact, the position of the second peak in the present $G_N^{inter}(r)$ roughly corresponds to this distance. The N···D_{W2} interaction should be involved in the second peak at the $G_N^{inter}(r)$. In order to reproduce the second peak of the present $G_N^{inter}(r)$, it was found to be necessary to take into account the contribution from another type of hydrogen bond, N–D···OD_2. Therefore, we concluded that the first hydration shell of the amino group in the present solution consists of two different kinds of hydrogen bonds, i.e., I) one of the deuterium atoms of the D_2O molecule is directly hydrogen-bonded to the amino-nitrogen atom. II) The oxygen atom of the other D_2O molecule is hydrogen-bonded to the amino-hydrogen atoms. These structural features are very similar to those reported for aqueous alkaline 2 mol % glycine solutions.[25] An additional indication of further structure can be recognized as the more broadened third and fourth peaks located at $r \approx 4$ and 5.5 Å.

In order to obtain the structural parameters concerning the hydration around the amino group, the least squares fitting analysis was applied to the observed $\Delta_N^{inter}(Q)$. The following assumptions were employed in evaluating the theoretical interference term. a) For the nearest neighbor N···D_{W1}–$O_W D_{W2}$ interaction, parameters $r_{ND_{W1}}$, $l_{ND_{W1}}$, $n_{ND_{W1}}$, and the bond angle α (=∠N···D_{W1}–O_W) were treated as independent parameters. The molecular geometry of D_2O was fixed to that reported for pure liquid D_2O ($r_{OD} = 0.983$ Å, $r_{DD} = 1.55$ Å).[22] Parameters l_{NO_W} and r_{NO_W} were allowed to vary independently, while n_{NO_W} and $n_{ND_{W2}}$ were fixed to the value of $n_{ND_{W1}}$ in the fitting procedure. The dihedral angle between the plane involving N···D_{W1}–O_W atoms and molecular plane of the D_2O, β, was also treated as an independent parameter. b) Structural parameters for the second nearest neighbor N···D_2O interaction, r_{NO}, l_{NO}, n_{NO}, r_{ND}, and l_{ND}, were refined independently, while the coordination number, n_{ND}, was fixed to the value of $2n_{NO}$. c) Contributions from the third and fourth nearest neighbor N···D_2O interactions were taken into account in the present model function in which each contribution was treated as a single interaction with the coherent scattering length in Eq. 3, b_α, being $2b_D + b_O$. d) The long-range parameters r_0 and l_0 were refined independently. The fitting procedure was carried out using the SALS program,[21] assuming that the statistical uncertainties distribute uniformly over the whole Q-range employed.

The best-fit result is compared with the observed $\Delta_N^{inter}(Q)$ in Fig. 1c. A satisfactory agreement is obtained between the observed and calculated $\Delta_N^{inter}(Q)$. The observed and calculated $G_N^{inter}(r)$ (Fig. 2b) also agree well with each other. The final results of all independent parameters are summarized in Table 4. The present value of the nearest neighbor N···D_{W1} interaction, $r_{ND_{W1}} = 2.00(1)$ Å and $n_{ND_{W1}} = 0.97(1)$, are in good agreement with those reported for the aqueous alkaline glycine solutions ($r_{ND_{W1}} = 1.97(3)$ Å and $n_{ND_{W1}} = 1.14(3)$),[25] indicating the formation of a hydrogen bond of N···D_{W1}–$O_W D_{W2}$ type. The present value of the N···D_{W1}–O_W angle, $\alpha = 165(10)^\circ$, implies that an almost linear hydrogen bond is present between the nitrogen atom and the nearest neighbor D_2O molecule. The N···O and N···D distances for the second nearest neighbor N···D_2O interaction are determined to be 2.95(5) and 3.35(5) Å, respectively. These values are in good agreement with those observed in the aqueous alkaline glycine solutions in which the amino group exists as the neutral form (–ND_2).[25] On the other hand, the present r_{NO} value for the N···D_2O(II) interaction is slightly larger than that reported for an aqueous 3 mol % alanine solution ($r_{NO} = 2.88(2)$ Å),[9] that for an aqueous 5 mol % glycine solution ($r_{NO} = 2.85(5)$ Å),[26] and that for an aqueous 2 mol % glycine solution in acidic condition ($r_{NO} = 2.90(2)$

Table 4. Results of the Least Squares Refinement for $\Delta_N^{inter}(Q)$ Observed for Aqueous 18 mol % Lithium Alaninate Solutions in D_2O[a)]

Interaction	i···j	r_{ij}/Å	l_{ij}/Å	n_{ij}
N···D_2O (I)	N···D_{W1}	2.00(1)	0.13(2)	0.97(1)
	N···O_W	—	0.14(2)	(0.97)[b)]
	N···D_{W2}	—	0.14(2)	(0.97)[b)]
		$\alpha = 165(10)^{\circ}$[c)]	$\beta = 10(5)^{\circ}$[d)]	
N···D_2O (II)	N···O	2.95(5)	0.20(5)	1.4(1)
	N···D	3.35(5)	0.20(4)	(2.8)[e)]
N···D_2O (III)	N···D_2O	4.00(5)	0.48(1)	5.3(7)
N···D_2O (IV)	N···D_2O	5.25(1)	0.72(1)	1.1(1)
		r_0/Å	l_0/Å	
Long-range	N···X[f)]	4.64(9)	0.46(8)	

a) Estimated standard deviations are given in parentheses. b) Fixed at the value $n_{N\cdots D_{W1}}$. c) Bond angle $\angle$N···D_{W1}–O_W. d) Dihedral angle between plane involving N···D_{W1}–O_W atoms and molecular plane of D_2O. e) Fixed at the value $2n_{NO}$. f) X: N, O, C, Li, H, and D.

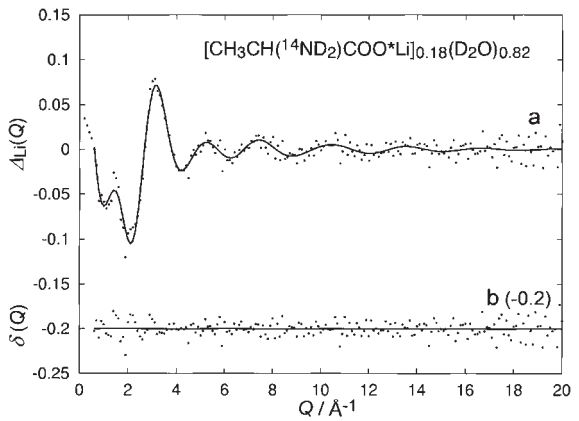

Fig. 3. a) Observed difference function, $\Delta_{Li}(Q)$, for aqueous 18 mol % lithium alaninate heavy water solutions (dots). The best-fit of calculated interference term (solid line). b) The residual function (dots).

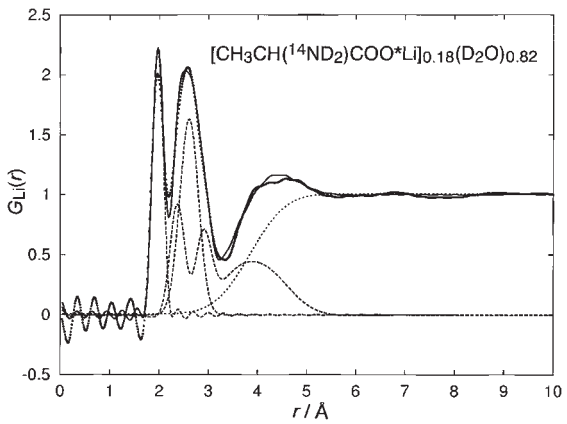

Fig. 4. Observed distribution function, $G_{Li}(r)$, around Li^+ (dots), and the Fourier transform of calculated $\Delta_{Li}^{model}(Q)$ (solid line). Short- and long-range contributions are denoted by broken and dotted lines, respectively.

Å),[27] in which the amino groups of the amino acid molecules have the cationic form (–ND_3^+). The tilt angle θ between the N···O axis and the molecular plane of the second nearest neighbor D_2O molecule is estimated to be 64(11)°.

Hydration Structure of the Lithium Ion. The observed difference function, $\Delta_{Li}(Q)$, and the corresponding distribution function around Li^+, $G_{Li}(r)$, are shown in Figs. 3 and 4, respectively. The interference feature of the present $\Delta_{Li}(Q)$ looks very similar to that reported for aqueous LiCl,[28–30] LiBr,[31,32] DCOOLi,[33] and C_6D_5COOLi[34] solutions. The present $G_{Li}(r)$ exhibits a common feature compared with that observed for aqueous solutions involving Li^+,[28–34] such as well-resolved Li^+–O and Li^+–D peaks located at $r \approx 2.0$ and 2.6 Å, respectively. This reflects the stable orientational correlation between Li^+ and the water molecules in the first hydration shell. The number of oxygen atoms around Li^+, n_{LiO}, was estimated to be 2.4 from the area under the first peak of the present $G_{Li}(r)$. However, the coordination number, n_{LiD}, evaluated from the second peak was found to be much larger than the expected value, $2n_{LiO}$. This implies that the contribution from the nearest neighbor Li^+···alaninate interaction is involved in the second peak of the present $G_{Li}(r)$.

In order to obtain more detailed structural information concerning the local structure around Li^+, the least squares fitting analysis was adopted for the observed $\Delta_{Li}(Q)$. Contributions from the nearest neighbor Li^+···D_2O, Li^+···alaninate ion, and long-range interactions were taken into account in evaluating the model function. The following assumptions were adopted: a) Parameters for internuclear distances, r_{LiO} and r_{LiD}, and their root-mean-square amplitudes, l_{LiO} and l_{LiD}, for the first hydration shell were refined independently. b) The coordination number, n_{LiO}, for the first hydration shell was treated as an independent parameter, while the value of n_{LiD} was fixed at $2n_{LiO}$. c) For the Li^+···alaninate interaction, the internuclear distance, r_{LiO_C}, its r.m.s amplitude, l_{LiO_C}, and the coordination number, n_{LiO_C}, were refined independently. The bond angle α (=$\angle Li^+\cdots O_C$–C) and the dihedral angle β between the plane involving $Li^+\cdots O_C$–C atoms and that involved in the carboxyl group (COO^-) of the alaninate ion, were treated as independent parameters. d) The r.m.s. amplitudes, l_{Lij}, for the non-bond-

Table 5. Results of the Least Squares Refinement for $\Delta_{Li}(Q)$ Observed for Aqueous 18 mol % Lithium Alaninate Solutions in D_2O[a)]

Interaction	i···j	r_{ij}/Å	l_{ij}/Å	n_{ij}
Li^+···D_2O	Li^+···O	1.97(1)	0.103(1)	2.42(5)
	Li^+···D	2.62(2)	0.19(1)	(4.84)[b)]
Li^+···alaninate	Li^+···O_C[c)]	2.38(1)	0.15(2)	2.3(2)
		$\alpha = 101(1)^\circ$[d)]	$\beta = 74(1)^\circ$[e)]	$l^* = 0.27(1)$ Å[f)]
		r_0/Å	l_0/Å	
Long-range	Li^+···X[g)]	3.93(2)	0.57(2)	

a) Estimated standard deviations are given in parentheses. b) Fixed at the value n_{LiO}. c) Carboxyl-oxygen atom within the alaninate ion. d) Bond angle $\angle Li^+\cdots O_C$–C. e) Dihedral angle between plane involving carboxyl group within the alaninate ion and plane involving $Li^+\cdots O_C$–C atoms. f) The r.m.s. parameter for non-bonding interactions in the Li^+···alaninate complex. See text for detail. g) X: N, O, C, Li, H, and D.

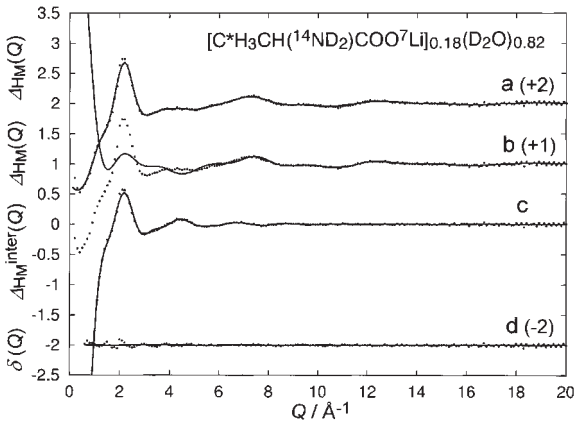

Fig. 5. a) Observed difference function, $\Delta_{H_M}(Q)$, for aqueous 18 mol % lithium alaninate heavy water solutions (dots). Smoothed $\Delta_{H_M}(Q)$, which is used for the Fourier transform (solid line). b) Observed $\Delta_{H_M}(Q)$ (dots), and the intramolecular interference term within the alaninate ion, $I_{H_M}{}^{intra}(Q)$ (solid line). c) Intermolecular difference function, $\Delta_{H_M}{}^{inter}(Q)$ (dots). The best-fit of the calculated $\Delta_{H_M}{}^{model}(Q)$ is shown by the solid line. d) The residual function, $\delta(Q)$ (dots).

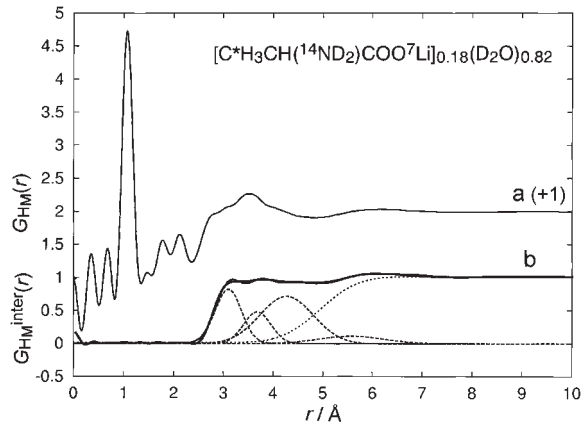

Fig. 6. a) Total distribution function around the methyl-hydrogen atom, $G_{H_M}(r)$, observed for aqueous 18 mol % lithium alaninate solutions. b) Observed intermolecular distribution function, $G_{H_M}{}^{inter}(r)$ (Thick solid line), and the Fourier transform of the calculated $\Delta_{H_M}{}^{model}(Q)$ (Fig. 5c) is shown by thin solid line. Short- and long-range contributions are denoted by broken and dotted lines, respectively.

ing interaction within the Li^+···alaninate complex were approximated by the following equation:[18]

$$l_{Lij} = l_{LiO_C}{}^* \times (r_{Lij}/r_{LiO_C})^{1/2}, \quad (6)$$

where $l_{LiO_C}{}^* = l_{LiO_C} + l^*$. In the present analysis, the r.m.s. amplitude was modified by an additional parameter, l^*, to improve the fit in the lower-Q region below $Q < 4$ Å^{-1}. e) Parameters r_0 and l_0 for the continuous long-range random distribution of atoms were refined independently.

The best-fit result is compared in Fig. 3. A satisfactory agreement is obtained in the range of $0.6 \le Q \le 20$ Å^{-1}. The final results of the least squares fit are summarized in Table 5. The present values of r_{LiO} and r_{LiD} for the nearest neighbor Li^+···D_2O interaction are in reasonable agreement with those reported in various aqueous solutions.[28–34] However, the present value of n_{LiO} (=2.42(5)) is much smaller than the value 4–6 found for more dilute aqueous LiCl[28–30] and LiBr[31,32] solutions in which Li^+ does not form contact ion pairs. The fact confirms that the first hydration shell of Li^+ involves the alaninate ion in the present solution. The intermolecular distance, r_{LiO_C}, and the coordination number, n_{LiO_C}, for the nearest neighbor Li^+···O_C interaction are determined to be 2.38(1) Å and 2.3(2), respectively. The present value of r_{LiO_C} is considerably smaller than that found in an aqueous 12 mol % DCOOLi solution ($r_{LiO_C} = 2.63(3)$ Å),[33] while the nearest neighbor coordination number, n_{LiO_C}, in the present solutions is twice as large as that reported for the DCOOLi solution ($n_{LiO_C} = 1.2(1)$).[33] Present values of the Li^+···O_C–C bond angle, α, and the dihedral angle, β, indicate that the configuration of one of the carboxyl-oxygen atoms of the alaninate ion faces towards Li^+. The first coordination shell of the Li^+ is found to consist of ca. 2.4 D_2O molecules and ca. 2.3 alaninate ions in the present solution.

Hydration Structure around the Methyl-Hydrogen Atom. The observed $\Delta_{H_M}(Q)$ shown in Fig. 5a exhibits the first diffraction peak at $Q \approx 2$ Å^{-1}, followed by a shoulder appearing at the lower-Q side and an oscillatory feature extending to the higher-Q region. The distribution function around the methyl-hydrogen atom, $G_{H_M}(r)$, is described in Fig. 6a.

Table 6. Results of the Least Squares Refinement for $\Delta_{H_M}{}^{inter}(Q)$ Observed for Aqueous 18 mol % Lithium Alaninate Solutions in D_2O[a)]

Interaction	i···j	r_{ij}/Å	l_{ij}/Å	n_{ij}
$H_M \cdots D_2O$ (I)	$H_M \cdots D_2O$	3.12(1)	0.26(1)	0.62(1)
$H_M \cdots D_2O$ (II)	$H_M \cdots D_2O$	3.70(1)	0.27(1)	0.51(1)
$H_M \cdots D_2O$ (III)	$H_M \cdots D_2O$	4.34(3)	0.54(1)	2.1(2)
$H_M \cdots D_2O$ (IV)	$H_M \cdots D_2O$	5.65(4)	0.65(4)	0.7(1)
		r_0/Å	l_0/Å	
Long-range	$H_M \cdots X$[b)]	5.01(7)	0.6(1)	

a) Estimated standard deviations are given in parentheses. b) X: N, O, C, Li, H, and D.

The dominant first peak at $r \approx 1.1$ Å is assigned to the intramolecular C–D bond of the methyl group in the alaninate ion. Intramolecular non-bonding interactions may be involved in the second and the third peaks at $r \approx 1.8$ and 2.2 Å.

In order to confirm the reliability of the present $\Delta_{H_M}(Q)$, the normalization factor, γ, was estimated by applying the same procedure as that adopted for the observed $\Delta_N(Q)$. The value obtained ($\gamma = 0.98 \pm 0.01$) indicates that the overall normalization error in the present $\Delta_{H_M}(Q)$ is estimated within ca. 2%. The calculated intramolecular contribution, $I_{H_M}{}^{intra}(Q)$ (Fig. 5b), was then subtracted from the observed $\Delta_{H_M}(Q)$ to obtain the intermolecular difference function as shown in Fig. 5c. The intermolecular distribution function, $G_{H_M}{}^{inter}(r)$ (Fig. 6b), around the methyl-hydrogen atom looks rather featureless, which suggests very weak interactions between the methyl-hydrogen atom and neighboring water molecules. However, an indication of the first hydration shell can be seen as a slightly resolved peak located at $r \approx 3$ Å.

A quantitative analysis of the observed $\Delta_{H_M}{}^{inter}(Q)$ was carried out by applying the least squares refinement using the model function as described in Eq. 3. It is difficult to make an unambiguous assignment of the peak observed in the present $G_{H_M}{}^{inter}(r)$, because contributions from both $H_M \cdots O_W$ and $H_M \cdots D_W$ interactions are involved in the $G_{H_M}{}^{inter}(r)$. In the present analysis, contributions from the first, second, and third hydration shells were taken into account, and each contribution was treated as a single interaction with the coherent scattering length in Eq. 3, b_α, being $2b_D + b_O$. The fitting procedure was performed by using the SALS program[21] in the range of $0.6 \leq Q \leq 20$ Å^{-1}.

The results of the least squares fit for the observed $\Delta_{H_M}{}^{inter}(Q)$ is represented in Fig. 5c. A satisfactory agreement is obtained between the observed and calculated $\Delta_{H_M}{}^{inter}(Q)$ in the whole Q-range. The final values of all independent parameters are summarized in Table 6. The present nearest neighbor $H_M \cdots D_2O$ distance (3.12(1) Å) is considerably longer than that of the nearest neighbor $H_M \cdots O_W$ interaction reported for an aqueous 3 mol % alanine solution (2.58(1) Å).[9] On the other hand, the present $H_M \cdots D_2O$ distance is in reasonable agreement with the nearest neighbor $H_M \cdots D_W$ distance (2.99(2) Å) found in the aqueous 3 mol % alanine solution.[9] Since the contribution from the $H_M \cdots D_W$ partial structure factor is twice as large as that from the $H_M \cdots O_W$ one in the present experimental condition, $G_{H_M}{}^{inter}(r)$ is dominated by the $H_M \cdots D_W$ interaction. In order to obtain more detailed information on the orientational correlation of water molecules in the first hydration shell of the methyl-hydrogen atom, it is necessary to derive the partial distribution functions, $g_{H_MO_W}(r)$ and $g_{H_MD_W}(r)$. This requires additional neutron diffraction measurements for sample solutions in which the H/D composition of the solvent molecule is changed.

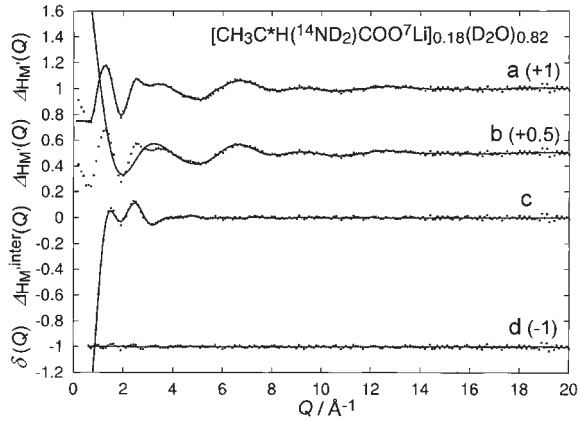

Fig. 7. a) Observed difference function, $\Delta_{H_{M'}}(Q)$, for aqueous 18 mol % lithium alaninate heavy water solutions (dots). Smoothed $\Delta_{H_{M'}}(Q)$, which is used for the Fourier transform (solid line). b) Observed $\Delta_{H_{M'}}(Q)$ (dots), and the intramolecular interference term within the alaninate ion, $I_{H_{M'}}{}^{intra}(Q)$ (solid line). c) Intermolecular difference function, $\Delta_{H_{M'}}{}^{inter}(Q)$ (dots). The best-fit of the calculated $\Delta_{H_{M'}}{}^{model}(Q)$ is shown by the solid line. d) The residual function, $\delta(Q)$ (dots).

Hydration Structure around the Methine-Hydrogen Atom. The observed difference function, $\Delta_{H_{M'}}(Q)$, and corresponding distribution function around the methine-hydrogen atom of the alaninate ion, $G_{H_{M'}}(r)$, are shown in Figs. 7a and 8a, respectively. The present $\Delta_{H_{M'}}(Q)$ is characterized by the first peak located at $Q \approx 1.3$ Å^{-1}, followed by an oscillatory feature extending to the higher-Q region. The dominant first peak at $r \approx 1.1$ Å is ascribed to the intramolecular $H_{M'} \cdots C_\alpha$ interaction. The sum of the contributions from $H_{M'} \cdots C_M$, $H_{M'} \cdots C_O$, and $H_{M'} \cdots N$ intermolecular non-bonding interactions appears as the second peak located at $r \approx 2.1$ Å in the present $G_{H_{M'}}(r)$. The reliability of the present $\Delta_{H_{M'}}(Q)$ was confirmed by estimating the normalization factor, γ, by applying the least squares fit of the intramolecular interference term $I_{H_{M'}}{}^{intra}(Q)$

to the observed $\Delta_{H_{M'}}(Q)$ in the range of $6 \leq Q \leq 20\,\text{Å}^{-1}$. The obtained value $\gamma = 0.98(1)$ implies that the present data correction and normalization procedures have been adequately carried out; the overall normalization uncertainty in the present $\Delta_{H_{M'}}(Q)$ is roughly estimated to be within 2%. The calculated $I_{H_{M'}}{}^{intra}(Q)$ was then subtracted from the observed $\Delta_{H_{M'}}(Q)$ to obtain the intermolecular difference function, $\Delta_{H_{M'}}{}^{inter}(Q)$, as shown in Fig. 7c. The corresponding distribution function around the methine-hydrogen atom, $G_{H_{M'}}{}^{inter}(r)$, is represented in Fig. 8b. The partially resolved peak located at $r \approx 3$ Å in the present $G_{H_{M'}}{}^{inter}(r)$ indicates that a weak hydration shell is present. An indication of the structural feature is observed as a broadened peak at $r \approx 5.5$ Å.

In order to obtain the structural parameters concerning the hydration of the methine-hydrogen atom, the least squares fitting analysis was applied to the observed $\Delta_{H_{M'}}{}^{inter}(Q)$. In the present analysis, the short-range $H_{M'}\cdots D_2O$ interaction was approximated as a single interaction with the value of b_α in Eq. 3 being $2b_D + b_O$. It has been found that at least four short-range interactions are necessary to reproduce the observed $\Delta_{H_{M'}}{}^{inter}(Q)$. Contributions from the long-range random distribution of atoms are taken into account. The best-fit result is compared with the observed $\Delta_{H_{M'}}{}^{inter}(Q)$ in Fig. 7c. The agreement between the observed and calculated $\Delta_{H_{M'}}{}^{inter}(Q)$ is satisfactory. The observed and calculated $G_{H_{M'}}{}^{inter}(r)$ (Fig. 8b) also agree well with each other. The final results of the least squares fit are summarized in Table 7. The present value of the average $H_{M'}\cdots D_2O$ distance, 2.87(3) Å, is larger than the sum of the van der Waals radius of the hydrogen atom and the effective radius of the water molecule ($1.2 + 1.4 = 2.6$ Å), suggesting a very weak interaction between the methine-hydrogen atom and D_2O molecule in the first hydration shell. The number of water molecules within the first hydration shell of the methine-hydrogen atom is obtained to be 0.86(9).

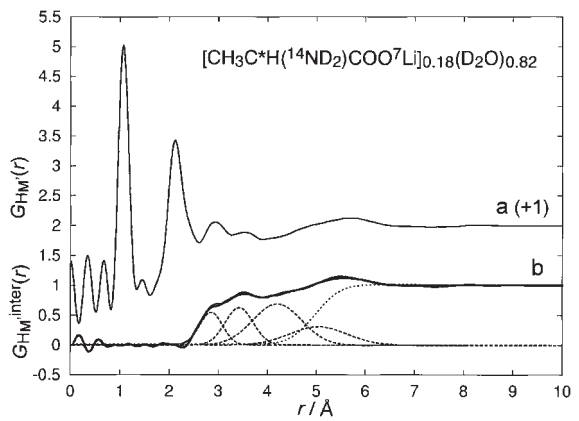

Fig. 8. a) Total distribution function around the methine-hydrogen atom, $G_{H_{M'}}(r)$, observed for aqueous 18 mol % lithium alaninate solutions. b) Observed intermolecular distribution function, $G_{H_{M'}}{}^{inter}(r)$ (Thick solid line), and the Fourier transform of the calculated $\Delta_{H_{M'}}{}^{model}(Q)$ (Fig. 7c) is shown by thin solid line. Short- and long-range contributions are denoted by broken and dotted lines, respectively.

In conclusion, information on the environmental structure around the amino-nitrogen, the methyl-hydrogen, and the methine-hydrogen atoms within the alaninate ion, and the coordination structure of the lithium ion in highly concentrated aqueous solution has been obtained. In the present solution, each Li^+ is surrounded by on the average ca. 2 water molecules and ca. 2 alaninate ions. The number of water molecules neighboring the alaninate ion is roughly estimated by the sum of the number of water molecules within the first hydration shell of the amino- (0.97 + 1.4), the methyl- (0.62 × 3), the methine- (0.86), and the carboxyl-group (unknown value, 1–2 in reasonable estimation), which corresponds to 6–7 water molecules; the value is considerably smaller than that obtained for the zwitterionic alanine molecule in more diluted aqueous solution (8–9).[9] Considering that ca. 2 water molecules are in the first coordination shell of Li^+, the total number of water molecules within the first coordination shell of both Li^+ and alaninate ion is approximately calculated to be 8–9, which is twice as large as the number of water molecules per one lithium alaninate. This implies that each water molecule is shared by on average two Li^+ or alaninate ions in the present highly concentrated solution.

The authors would like to acknowledge Prof. Toshiharu Fukunaga (Kyoto University) and Dr. Keiji Itoh (Kyoto University) for their help during the course of neutron diffraction measurements. All calculations were carried out at the Yamagata University Networking and Computing Service Center. This work was partially supported by Grant-in-Aid for Scientific Research on Priority Areas (No. 16041205), Scientific Research (C) (No. 16550049), and Creative Scientific Research (No. 16GS0417), from the Ministry of Education, Culture, Sports, Science and Technology.

Table 7. Results of the Least Squares Refinement for $\Delta_{H_{M'}}{}^{inter}(Q)$ Observed for Aqueous 18 mol % Lithium Alaninate Solutions in D_2O[a)]

Interaction	i···j	r_{ij}/Å	l_{ij}/Å	n_{ij}
$H_{M'}\cdots D_2O$ (I)	$H_{M'}\cdots D_2O$	2.87(3)	0.233(1)	0.86(9)
$H_{M'}\cdots D_2O$ (II)	$H_{M'}\cdots D_2O$	3.45(3)	0.28(2)	1.72(4)
$H_{M'}\cdots D_2O$ (III)	$H_{M'}\cdots D_2O$	4.26(4)	0.49(1)	5.0(4)
$H_{M'}\cdots D_2O$ (IV)	$H_{M'}\cdots D_2O$	5.65(4)	0.65(4)	0.7(1)
		r_0/Å	l_0/Å	
Long-range	$H_{M'}\cdots X$[b)]	5.01(7)	0.6(1)	

a) Estimated standard deviations are given in parentheses. b) X: N, O, C, Li, H, and D.

References

1 S. H. Laurie, *Comprehensive Coordination Chemistry*, ed. by G. Wilkinson, Pergamon Press, Oxford, **1987**, Vol. 2, p. 739.

2 K. Ozutsumi, H. Ohtaki, *Bull. Chem. Soc. Jpn.* **1983**, *56*, 3635.

3 K. Ozutsumi, H. Ohtaki, *Bull. Chem. Soc. Jpn.* **1984**, *57*, 2605.

4 K. Ozutsumi, H. Ohtaki, *Bull. Chem. Soc. Jpn.* **1985**, *58*, 1651.

5 K. Ozutsumi, T. Yamaguchi, H. Ohtaki, K. Tohji, Y. Udagawa, *Bull. Chem. Soc. Jpn.* **1985**, *58*, 2786.

6 T. Radnai, K. Inoue, H. Ohtaki, *Bull. Chem. Soc. Jpn.* **1990**, *63*, 3420.

7 F. Jensen, *J. Am. Chem. Soc.* **1992**, *114*, 9533.

8 R. V. Krishnakumar, M. S. Nandhini, S. Natarajan, K. Sivakumar, B. Varghese, *Acta Crystallogr., Sect. C* **2001**, *57*, 1149.

9 Y. Kameda, K. Sugawara, T. Usuki, O. Uemura, *Bull. Chem. Soc. Jpn.* **2003**, *76*, 935.

10 T. Fukunaga, M. Misawa, I. Fujikura, S. Satoh, *KENS Report-IX*, **1993**, p. 16.

11 H. H. Paalman, C. J. Pings, *J. Appl. Phys.* **1962**, *33*, 2635.

12 I. A. Blech, B. L. Averbach, *Phys. Rev.* **1965**, *137*, A1113.

13 V. F. Sears, *Neutron News* **1992**, *3*, 26.

14 J. R. Granada, V. H. Gillete, R. E. Mayer, *Phys. Rev. A* **1987**, *36*, 5594.

15 Y. Kameda, M. Sasaki, T. Usuki, T. Otomo, K. Itoh, K. Suzuya, T. Fukunaga, *J. Neutron Res.* **2003**, *11*, 153.

16 A. K. Soper, G. W. Neilson, J. E. Enderby, H. A. Howe, *J. Phys. C: Solid State Phys.* **1977**, *10*, 1793.

17 J. E. Enderby, G. W. Neilson, *Water: A Comprehensive Treatise*, ed. by F. Franks, Prenum Press, New York, **1979**, Vol. 6, p. 1.

18 A. H. Narten, M. D. Danford, H. A. Levy, *Discuss. Faraday Soc.* **1967**, *43*, 97.

19 R. Caminiti, P. Cucca, M. Monduzzi, G. Saba, G. Crisponi, *J. Chem. Phys.* **1984**, *81*, 543.

20 H. Ohtaki, N. Fukushima, *J. Solution Chem.* **1992**, *21*, 23.

21 T. Nakagawa, Y. Oyanagi, *Recent Development in Statistical Inference and Data Analysis*, North-Holland, **1980**, p. 221.

22 Y. Kameda, O. Uemura, *Bull. Chem. Soc. Jpn.* **1992**, *65*, 2021.

23 H. J. Simpson, Jr., R. E. Marsh, *Acta Crystallogr.* **1966**, *20*, 550.

24 K. Iijima, B. Beagley, *J. Mol. Struct.* **1991**, *248*, 133.

25 K. Sugawara, Y. Kameda, T. Usuki, O. Uemura, T. Fukunaga, *Bull. Chem. Soc. Jpn.* **2000**, *73*, 1967.

26 Y. Kameda, H. Ebata, T. Usuki, O. Uemura, M. Misawa, *Bull. Chem. Soc. Jpn.* **1994**, *67*, 3159.

27 K. Sugawara, Y. Kameda, T. Usuki, O. Uemura, *J. Phys. Soc. Jpn.* **2001**, *70*, Suppl. A, 365.

28 J. R. Newsome, G. W. Neilson, J. E. Enderby, *J. Phys. C: Solid State Phys.* **1979**, *13*, L923.

29 M. Yamagami, T. Yamaguchi, H. Wakita, M. Misawa, *J. Chem. Phys.* **1994**, *100*, 3122.

30 I. Howell, G. W. Neilson, *J. Phys.: Condens. Matter* **1996**, *8*, 4455.

31 Y. Kameda, O. Uemura, *Bull. Chem. Soc. Jpn.* **1993**, *66*, 384.

32 Y. Kameda, S. Suzuki, H. Ebata, T. Usuki, O. Uemura, *Bull. Chem. Soc. Jpn.* **1997**, *70*, 47.

33 Y. Kameda, T. Usuki, O. Uemura, *High Temp. Mater. Processes (London)* **1999**, *18*, 27.

34 Y. Kameda, K. Mochiduki, M. Imano, H. Naganuma, M. Sasaki, Y. Amo, T. Usuki, *J. Mol. Liq.* **2005**, *119*, 159.